Journal of Nuclear Materials 386–388 (2009) 8–14

Contents lists available at ScienceDirect

Journal of Nuclear Materials

journal homepage: www.elsevier.com/locate/jnucmat

Advances in microstructural characterization

S.J. Zinkle [a,*], G.E. Ice [a], M.K. Miller [a], S.J. Pennycook [a], X.-L. Wang [b]

[a] Materials Science and Technology Division, Oak Ridge National Laboratory, P.O. Box 2008, Oak Ridge, TN 37831, USA
[b] Neutron Scattering Science Division, Oak Ridge National Laboratory, P.O. Box 2008, Oak Ridge, TN 37831, USA

A B S T R A C T

Timely development of materials for the demanding fusion energy environment requires a broad range of advanced scientific tools, including advanced structural characterization methods. The current state-of-the-art and emerging capabilities in electron microscopy, atom probe tomography, neutron scattering and X-ray scattering are reviewed with respect to potential applications in fusion materials research and development. Recent dramatic advances in capabilities in all four of these characterization tools are transforming the spatial precision and quantitative information that can be extracted during structural characterization. Examples include spectroscopic identification of single atoms in bulk materials, three-dimensional mapping of millimeter-scale volumes of materials with nanometer resolution, and high-resolution in situ measurements of internal stress and strain during mechanical testing.

© 2008 Elsevier B.V. All rights reserved.

1. Introduction

Structural materials for future fusion energy systems must successfully function under simultaneous prolonged exposure to intense high-energy fluxes of neutrons, high heat fluxes (approaching those experienced by the space shuttle during reentry to the earth's atmosphere), high thermomechanical stresses, temperatures that may exceed half of the material's melting point, and coolant fluids that may be corrosive [1–3]. Several alloys containing a high density of uniformly-dispersed, highly-stable nanoscale precipitates or solute clusters are considered to be particularly attractive candidates for structural applications due to simultaneous achievement of high thermal creep strength and strong resistance to radiation-induced property degradation [4]. Since the initiating sequence of events that may lead to irradiation-induced phase instabilities or property degradation is often associated with atomic-scale mechanisms (e.g., precipitate dissolution or localized solute segregation at interfaces), there is strong interest in advanced structural and chemical characterization methods that can clarify these critical mechanisms.

Materials characterization involves three fundamental questions: what is the elemental composition, what are the crystal and local structures, and what types of defects are present. Dramatic advances in structural and chemical characterization tools that have been developed within the international materials science research community over the past few years are providing unprecedented fidelity in spatial resolution. In the following sections, the current status for electron microscopy, atom probe tomography, X-ray and neutron scattering tools are summarized.

2. Electron microscopy

Spurred on by the enormous versatility of electron microscopy, steady improvement in spatial resolution and a variety of spectroscopy tools have been achieved over the past few decades. Widely available capabilities now include energy-filtered electron energy loss spectroscopy (EELS) and sub-nanometer diameter probe energy dispersive spectroscopy that can provide detailed information on the chemical segregation of solute to interfaces and the composition of precipitates, along with a broad range of electron diffraction conditions that provide crystallographic space group and lattice parameter information. These new capabilities are routinely being used to provide detailed characterization on advanced materials of interest for fusion energy applications, including nanocomposited oxide dispersion strengthened ferritic alloys [5,6] and vanadium alloys [7].

In the last few years transmission electron microscopy has seen a rate of instrumental advance unheard of since the invention of the microscope in the 1930s, as shown in Fig. 1 [8]. Whereas optical microscopes have been operating near the resolution limit set by the wavelength of light for over 100 years, the achievable resolution of electron microscopes was limited to more than 50 times the electron wavelength through the end of the 20th century. This recent resolution breakthrough has been enabled by the successful correction of the dominant aberrations present in electron lenses [9,10]. It has also been aided by placing the microscopes in specialized rooms isolated from humans, vibration, electromagnetic fields and thermal gradients. Resolution has now crossed well into the sub-Ångstrom regime [11]. The benefits are much greater, however, than just the ability to resolve smaller atomic distances. It is now possible to image individual heavy atoms on surfaces [12,13] and inside a bulk material

* Corresponding author.
E-mail address: zinklesj@ornl.gov (S.J. Zinkle).

0022-3115/$ - see front matter © 2008 Elsevier B.V. All rights reserved.
doi:10.1016/j.jnucmat.2008.12.302

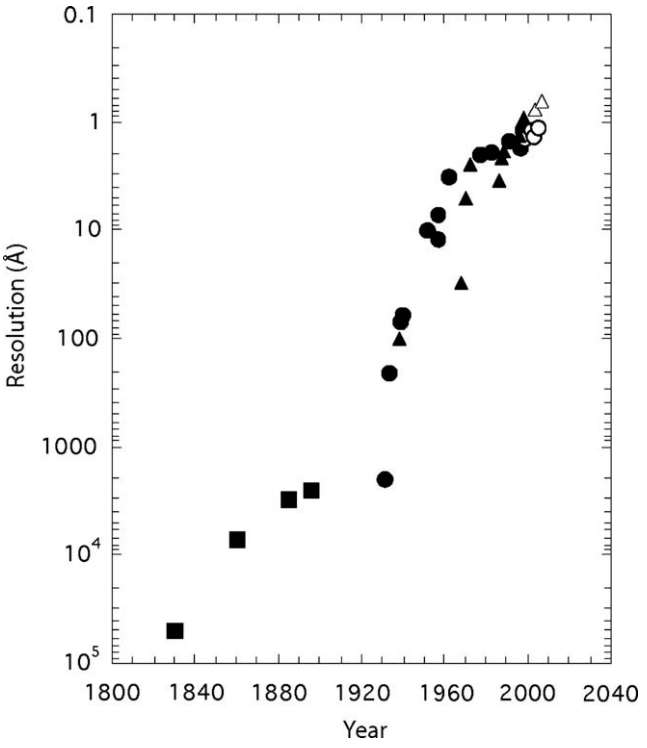

Fig. 1. The evolution of resolution; squares represent light microscopy, circles TEM, triangles STEM, solid symbols before aberration correction, open symbols after correction (after H. Rose, adapted from [8]).

[14,15], even to perform a spectroscopic identification of a single atom [16]. These instrumental advances allow new insights into longstanding issues in materials research, as reviewed elsewhere [17–19].

The main objective lens in an electron microscope is a round lens, which has an intrinsically high spherical aberration, of the order of 50 wavelengths compared to the roughly one wavelength typical of a light optical lens. The high aberration is due to physics [20], not poor quality components. Scherzer proposed the first design for an aberration corrector by relaxing one of these physics conditions, specifically by breaking the rotational symmetry of the system [21]. The major reason that this has taken over four decades to achieve is essentially instrumental, the need for highly-stable electronics and the need to tune all 40 or more optical elements individually. In the era of fast computers and efficient charge-coupled-device detectors, it is now possible to measure and correct aberrations iteratively in a process called autotuning, essentially a multidimensional form of autofocusing.

There are presently two designs of aberration corrector available for electron microscopes, a quadrupole/octapole design exclusively used in scanning transmission electron microscopy (STEM) and a hexapole design used in both STEM and transmission electron microscopy (TEM). These correctors are able to shape the electron wave front to a degree of perfection better than a quarter wavelength (~0.5 pm) over 70 microns, a level of performance that exceeds that of the Hubble Space Telescope. However, the correctors only compensate for the geometric aberrations of electron lenses, not for any chromatic aberration, which is the focusing of electrons of different energies at different points. Chromatic aberration correction has been successfully demonstrated so far only for scanning electron microscopy (SEM) [22] which operates at significantly lower accelerating voltages. Efforts are currently underway to extend this correction to the higher accelerating voltages normally needed for TEM [8].

The normal STEM imaging mode uses an annular dark field (ADF) detector that collects a large fraction of the scattered electrons [23]. If the inner detector angle is sufficiently high, the scattered intensity varies approximately as Z^2, where Z is the atomic number. This mode of operation provides a High Angle ADF image, commonly referred to as a Z-contrast image. One of the key advantages of STEM has always been the ability to have simultaneous detection of a variety of signals, for example, simultaneous Z-contrast and bright field images that allow pixel to pixel correlation. Replacing the bright field detector with an electron spectrometer, simultaneous Z-contrast imaging and electron energy loss spectroscopy becomes possible. The first demonstration of atomic resolution chemical analysis was in 1993, with spectra taken plane by plane across an atomically abrupt interface [24]. Later, it became routine to perform column-by-column spectroscopy [25]. Now, aberration correction has enabled dramatic gains in sensitivity due to the availability of smaller probes containing the same current. More current can channel down an atom column of interest with less wasted illumination of neighboring columns. This has allowed the first spectroscopic identification of a single atom inside a bulk material, as shown in Fig. 2 [16]. Recently, the first true two-dimensional spectroscopic maps have been obtained that show atomic resolution [26,27]. In addition, just as with X-ray absorption spectroscopy, the fine structure at an absorption edge gives an indication of the local electronic structure.

One of the unanticipated advantages of aberration correction has been the greatly reduced depth of field, which opens the possibility for three-dimensional (3D) imaging. Similar to a camera aperture, the depth of field decreases as the inverse square of the aperture angle. Although the aperture angles are still quite small by light optical standards, the typical depth of field has reduced dramatically as a result of aberration correction, becoming less than the thickness of a typical TEM specimen. Therefore, electron microscopy no longer provides the simple two-dimensional projection that it did in the past. Now, a through focal series becomes a through depth series of images, providing three-dimensional information on the specimen with depth resolution at the scale of a few nanometers and atomic resolution laterally [28]. A spectacular example of this capability is shown in Fig. 3 in which individual Hf atoms in a sub-nm wide region of SiO_2 in a high-dielectric constant semiconductor device have been located to a precision of about $0.1 \times 0.1 \times 1$ nm [29]. At present, this approach is limited to amorphous regions since in crystals electron channeling tends to work against bringing the beam to focus at a specific depth [30]. Also, achieving a depth resolution at the atomic level is not likely to be feasible in a single focal series. It will be necessary to use a combination of the conventional tilt series method with the optical sectioning approach, essentially a number of through focal series at different angles.

The next generation of aberration correctors are now beginning to appear, correcting all geometric aberrations up to 5th order. Another jump in resolution is anticipated, to the level of 0.5 Å, with a concomitant increase in single atom sensitivity and depth resolution. It should become possible to probe single impurity atoms at grain boundaries and dislocation cores, to probe their electronic environment and link it to macroscopic mechanical and electronic properties in a rigorous manner. With these new eyes, it should finally become possible to see the ultimate atomic origins of materials properties.

Another important development is the area of in situ observation stages. It is now routinely possible to obtain high-resolution images of nanoscale defect cluster motion during straining in an electron microscope at a wide range of temperatures (e.g., [31,32]). There is considerable activity underway to develop improved specimen stages that will enable high-resolution imaging

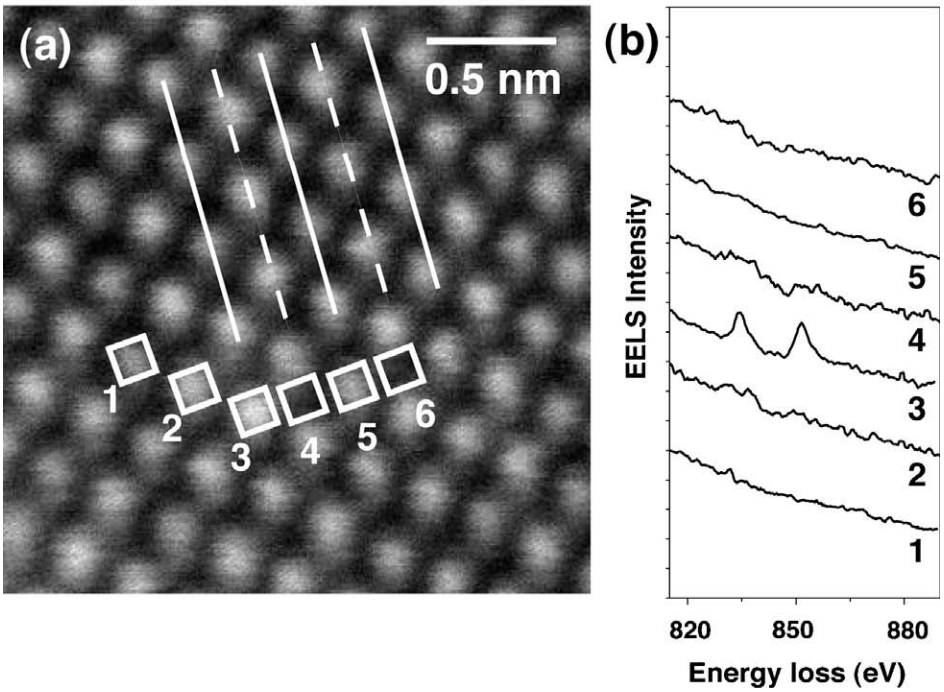

Fig. 2. Spectroscopic identification of an individual atom in its bulk environment by EELS. (a) Z-contrast image of $CaTiO_3$ showing traces of the CaO and TiO_2 {1 0 0} planes as solid and dashed lines respectively. A single La dopant atom in column 3 causes this column to be slightly brighter than other Ca columns, and EELS from it shows a clear La $M_{4,5}$ signal (b) Moving the probe to adjacent columns gives reduced or undetectable signals (adapted from [16]).

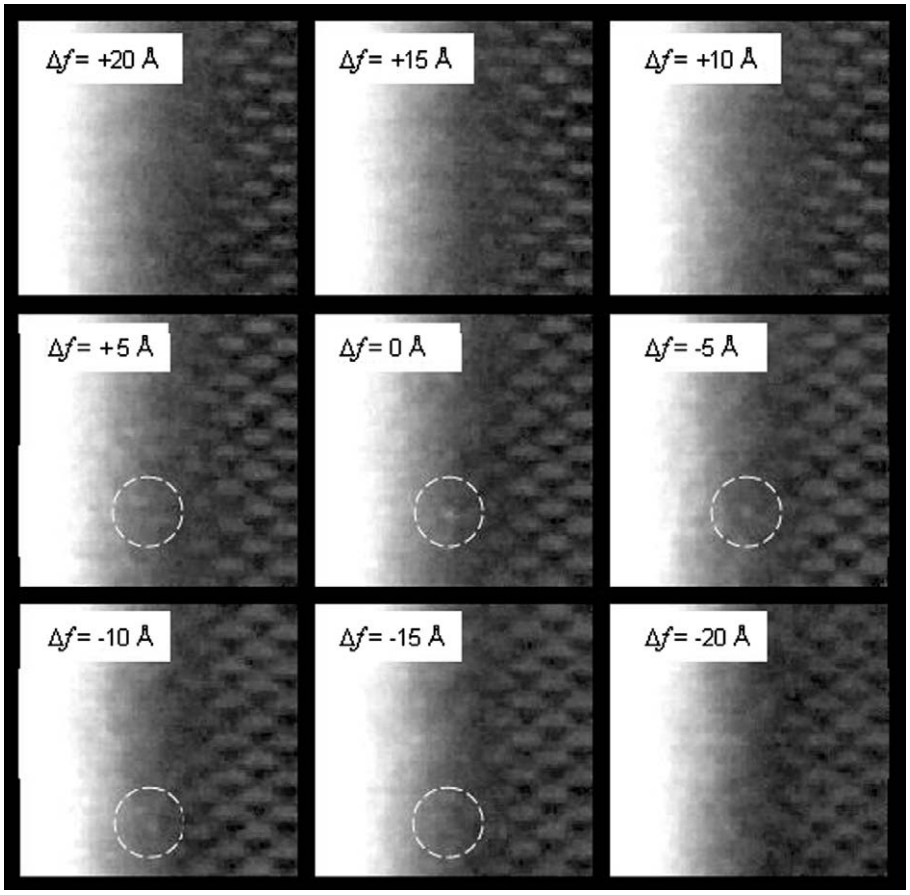

Fig. 3. A series of frames from a through focal series of images, recorded with 0.5 nm focal steps, showing the appearance and disappearance of an individual Hf atom (circled) in a thin layer of SiO_2 between the HfO_2 dielectric (left) and the Si gate region (right) (from [29]).

to be obtained during exposure of the sample to gaseous or liquid environments at a range of temperatures and pressures.

3. Atom probe tomography

Over the last decade, several transformational improvements have been made to atom probe tomography [33,34]. The use of a replaceable 20–50 μm-diameter local electrode in close proximity to the apex of the needle-shaped specimen enables the use of lower voltages to field evaporate atoms from the specimen. Lower voltage permits the pulse repetition rate of the field evaporation pulse to be increased from 1 to 2 kHz to over 200 kHz to dramatically reduce the data acquisition time. The local electrode atom probe (LEAP®) is also equipped with a wide area crossed delay line type of single atom, position-sensitive detector to increase the field of view [33]. These improvements have increased the volume of material that may be collected from a specimen. Typical datasets now contain between 5 and 100 million atoms. Newly developed focused ion beam based specimen preparation methods enable atom probe specimens to be fabricated from site specific locations, a wider range of materials, and may also reduce the volume and hence the activity of radioactive samples [35]. Although primarily driven by the need to quantify dopant profiles in semiconductors [33], the reintroduction of laser-assisted field evaporation [36] with more reliable pulsed picosecond and femtosecond lasers enables low electrical conductivity materials, including SiC [37] and zirconium alloys, to be characterized. In addition, laser-assisted field evaporation has benefits for the analysis of brittle materials due to the lower stress that is applied to the specimen. Most recently, the incorporation of a wide acceptance angle reflectron in the mass spectrometer improves the mass resolution so that the base of the mass peaks of all the isotopes can be separated in most materials. This higher resolution reduces the complexity of peak deconvolution and background noise subtraction for more reliable concentration measurements. During the last decade, significant advances have been made in the quantification of three-dimensional atom probe data [33]. In particular, friends-of-friends methods have been developed to quantify the size, number density and composition of nanoscale clusters, precipitates and solute segregation to dislocations [34,38,39], and the isoconcentration-based proximity histogram method has been developed to estimate solute profiles across interfaces and grain boundaries [40].

A typical example of the type of microstructural characterization that may be performed with the local electrode atom probe is shown in Fig. 4 for a mechanically alloyed, oxide dispersion strengthened (MA/ODS) 14YWT ferritic steel that was annealed for 1 h at 1000 °C and cold worked. These 10-nm-thick atom maps selected from the larger volume of analysis containing almost 10 millions atoms reveal a high number density of ~4-nm-diameter Ti-, Y- and O-enriched nanoclusters both in the ferrite matrix and also decorating the grain boundaries. The W was enriched to a level of 5.0 ± 0.2 at.% over a 2.7 nm wide (full width half maximum) region centered on the upper grain boundary. Lower levels of Cr and C segregation to the grain boundaries were also observed. The stability of the nanoclusters are responsible for the remarkable high temperature mechanical properties of these ODS alloys [5].

4. Advanced X-ray characterization

X-ray characterization of materials is being revolutionized by the ongoing development of intense synchrotron sources with orders-of-magnitude greater flux and brilliance (photons/s/μm^2/mrad^2) than conventional sources. Over the last 35 years, achievable X-ray source brilliance has increased by approximately 14 orders of magnitude [41]. As brilliance is the figure-of-merit for most characterization methods, this has enabled powerful new techniques that were previously impractical. For example, the energy-tunability of X-ray beams from early (first-generation) synchrotron sources fostered the development of absorption-fine-structure methods that can determine the local chemistry, near-neighbor atomic co-ordination and bond distances for dilute elements in crystalline or amorphous materials [42]. Similarly, the availability of intense. highly-collimated radiation from second-generation synchrotron sources enabled new surface diffraction and microfluorescence probes [43]. The stability of second-generation sources also allowed for widespread use of X-ray scattering contrast altering methods and/or near-resonance and absorption contrast techniques that highlight specific atoms in absorption or scattering [44,45].

The success of high-brilliance X-ray sources has also stimulated a renaissance in X-ray optics and detectors. These developing X-ray tools leveraged with vastly more powerful sources provide even more characterization opportunities. For example, high-performance X-ray focusing optics are rapidly developing and an international race for the smallest focal-spot size is underway. In the last decade, the achievable focal-spot area has decreased by more than two orders of magnitude [46]; ~2.5×10^5 nm^2 to ~600 nm^2. Small diameter X-ray beams allow for spatially-resolved measurements with resolution sufficient to resolve inhomogeneities in most real materials. Coupled with intense sources that provide sufficient flux into small phase-space volumes, it is now possible to perform experiments on submicron samples that once required mm or cm sized samples [47]. Similarly, fast and efficient area detectors have emerged that parallelize data collection for fast data

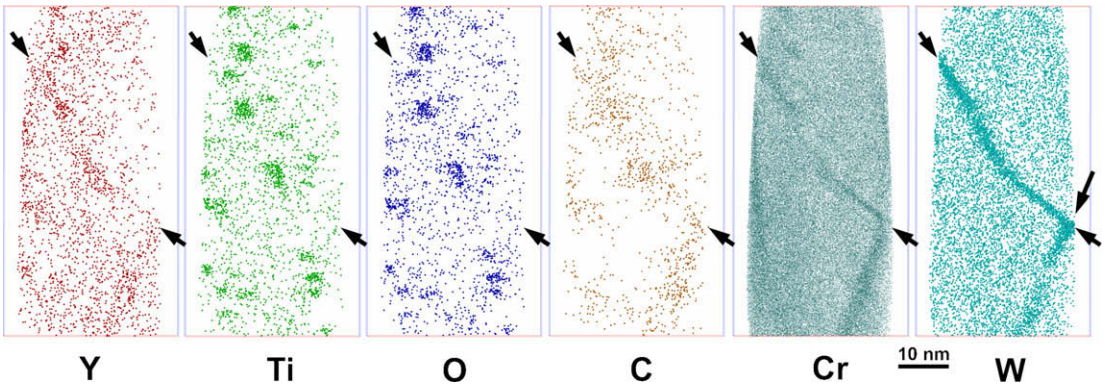

Fig. 4. Atom maps of the non-uniform solute distribution in mechanically alloyed, oxide dispersion strengthened 14YWT ferritic alloy that was annealed for 1 h at 1000 °C and cold worked. A high number density of ~4-nm-diameter Ti-, Y- and O-enriched nanoclusters are evident both in the ferrite matrix and also decorating the Cr-, W- and C-enriched grain boundaries (arrowed).

acquisition and reduced sample damage. These detectors can be used to make millisecond to femtosecond measurements. Furthermore, new detectors under development will integrate spectroscopy into area detection for improved experimental signal-to-noise and additional new characterization opportunities.

Although powerful characterization methods based on synchrotron sources are already deployed at facilities around the world, there are currently three directions of intense activity that will further extend opportunities for materials characterization. These areas can be summarized as (1) spatially-resolved methods for 3 D mapping of materials properties; (2) phase contrast and coherent imaging methods for the study of structures in thick samples and for nm resolution of 3 D structures [48], and (3) high-energy experiments that enable nondestructive measurements of local strain, texture and phase distributions in cm thick samples and for precision analysis of point and other defects [49]. All three of these methods are interrelated and ultimately based on a need to understand how real materials are organized in three dimensions and at different length scales.

Polychromatic microdiffraction, which is one important example of emerging spatially-resolved methods [50], allows for nondestructive characterization of local phase, crystal orientation, elastic strain and dislocation tensor distributions in 3 D with submicron resolution. Together with microfluorescence, it allows scientists to nondestructively map chemistry *and* local crystal structures to provide new insights into materials behavior. For example, Fig. 5 summarizes an improved data analysis of recent measurements that provided the first 3 D maps of grain-growth to test state-of-the art growth models [51]. The measurements not only quantify grain boundary types, curvatures and grain size, but also characterize local defect density and provide guidance on the role of defects in grain boundary migration. Other experiments have recently studied deformation behavior and the role of crystalline anisotropy and free surfaces, grain boundaries, and other symmetry breaking structures on local deformation behavior. These studies will guide next generation materials models.

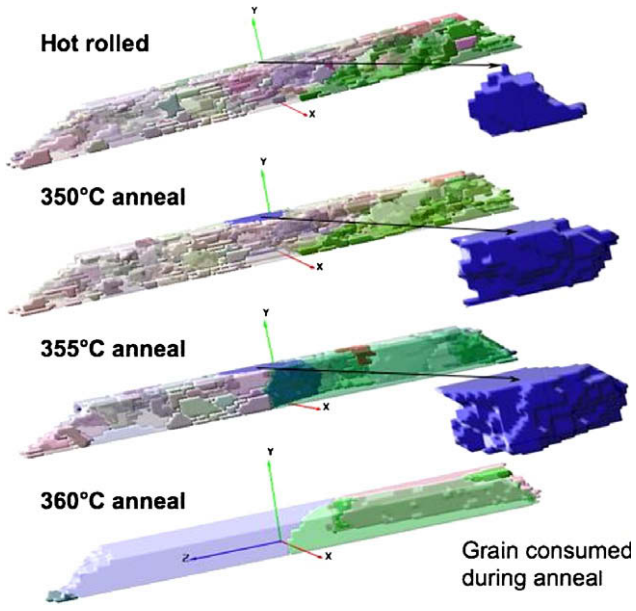

Fig. 5. Nondestructive μm-resolution 3 D false color images of local crystal orientations in an aluminum polycrystal at various heat treatment stages (1 h anneals). The analyzed depth in the images is about 10 μm. The observed grain boundary migration patterns require input of the local defect content of the neighbor grains which is simultaneously measured. This new information will guide a next generation of grain-growth theory. Beyond this early demonstration experiment, images with 100× larger fields of view will soon be available.

In the development of advanced nuclear materials, there are a number of situations with an obvious need for advanced X-ray characterization methods. For example, at the interface of dissimilar materials, spatially-resolved measurements of phase and elemental distributions can provide important new information about interface phase evolution. Similarly, measurements of damage and defect evolution in irradiated materials can now be carried out on polycrystalline samples with μm-sized grains. This will enable studies of real materials and the role of grain boundaries, crystalline orientation and other inhomogeneities in defect organization and will simplify measurements by using small-volume samples with orders of magnitude lower activity than traditional specimens. In addition, studies of mesoscale structure evolution during processing will guide the development of new grain boundary engineered and other high-performance materials.

Ultimately, emerging real-time, high-resolution images of 3 D materials properties will enable a new kind of materials exploration where scientists can move through a virtual sample with critical materials parameters encoded in the visualization. As advanced characterization techniques provide detailed tensor information in three dimensions, fundamentally new ways of visualizing data will be required to take full advantage of this emerging technology.

5. Neutron scattering

One of the unique features of the neutron scattering technique is the deep penetration compared to electrons and X-rays. For laboratory-sized samples, the measurements are therefore representative of the bulk rather than from surface areas. Moreover, sample environments can be readily implemented to allow in situ examination of structure evolution under extreme conditions. Because neutrons can penetrate deep inside most materials, a volumetric spatial mapping technique has been developed as a non-destructive means to determine residual stress or damage inside industrial-sized components [52].

Neutrons have wavelengths on the order of 1–10 Å, which is ideally suited for characterizing the structure of materials. Local atomic structures (e.g., atomic positions within a crystal lattice) are probed by wide-angle diffraction, whereas nano-scale microstructures are determined by small-angle neutron scattering (SANS) in the forward direction. The latter has proven to be particularly useful in the study of precipitation or phase transformation in alloys, such as in situ observation of the formation of nanocrystalline phases in multi-component metallic glass [53] and investigation of nanoscale solute clusters in unirradiated and irradiated steels [54–57]. Numerous studies have utilized SANS and complementary measurements such as TEM, positron annihilation spectroscopy [56] or APT [54,57] to provide detailed quantitative characterization of nanoscale solute clusters in steels. A recent SANS study has found that magnetic spin misalignment effects must be considered for detailed quantitative analyses of precipitates in steels [58]. SANS has also been used to study the microstructure in oxide-dispersion-strengthened (ODS) steel [59], which exhibits a dramatic improvement in thermal creep strength compared to conventional steels. Strong SANS intensity has been identified as arising from scattering from the nanoclusters formed during processing. Recent in situ SANS experiments confirmed earlier atom probe tomography observations [60] that these nanoclusters are stable up to 1400 °C.

Because the diffraction peak positions are related to inter-planar lattice spacing, this has inspired a new application that uses diffraction peaks as an internal strain gauge to characterize the mechanical behavior of materials. For a recent review, see Ref. [61]. In this method, strains are determined from the shift of the Bragg positions. Three-dimensional residual stress mapping

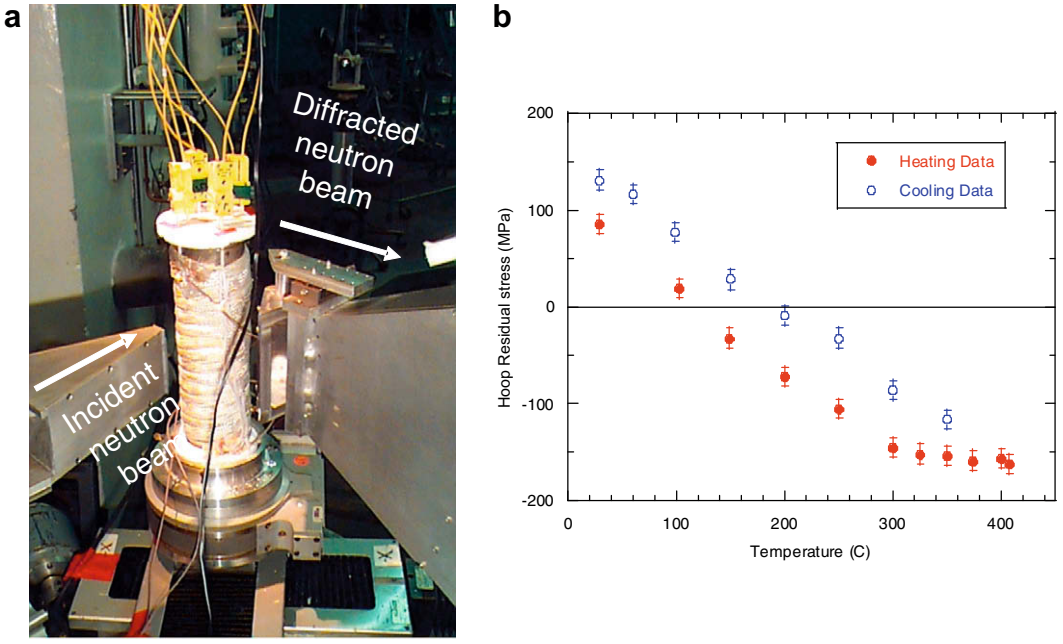

Fig. 6. (a) Experimental setup of an in situ experiment to determine the evolution of residual stress in a composite tube made of a carbon steel core and 304 L stainless steel clad. The tube was wrapped with heating tape and temperature monitored with a number of thermal couples around the circumference. The measurements were made inside the stainless 304 L steel clad layer. (b) Evolution of hoop (circumferential) stress during a thermal cycle. Upon heating, the hoop stress decreases linearly due to thermal expansion mismatch between carbon steel core and 304 L clad layer. The deviation from linear decrease upon heating above 300 °C indicates the onset of plasticity. Plastic deformation at elevated temperatures leads to higher residual stress upon cooling to room temperature.

is now routine and has made a significant impact on industrial applications. As an example, the development of residual stress in the clad layer of a steel tube at elevated temperature is shown in Fig. 6. This research was part of a study to improve the safety and longevity of recovery boilers used in the paper industry [62,63]. Plastic deformation occurred when temperatures reached 300 °C, as evidenced by the inflection point in the hoop stress data. These experimental data were essential for the selection of replacement materials in recovery boilers used in the paper industry.

While much of the early work was strongly oriented towards mechanical engineering, involving the determination of the residual stress distribution and the use of residual stress data in design and life prediction, opportunities for fundamental research began to emerge when it became evident that some of the experimental data could not be understood within the framework of the continuum theory and simple thermal-mechanical simulations [64]. For example, in situ measurements of the grain-orientation-dependent intergranular strains during uniaxial loading have been extensively used to identify the deformation mechanisms in polycrystalline materials [65]. Recently, this type of measurement has been extended to materials subject to cyclic loading [66] to study the damage mechanism by fatigue.

The construction of new sources and the upgrade of existing instruments bring new research opportunities. The Spallation Neutron Source at the Oak Ridge National Laboratory was commissioned in 2006 and by the end of 2008 it is scheduled to provide the world's most intense pulsed neutron beam (1.4 MW) for materials research. The high flux will make it possible to carry out in situ time-resolved measurements to study transient behavior. Simultaneous wide-angle diffraction and small-angle scattering will be particularly useful to examine structure evolution at multiple length scales during exposure to mechanical stress or chemical environments [67]. In situ wide-angle and small-angle scattering measurements of phase transformation kinetics at local and nano length scales are expected to shed light on classic problems in materials science, such as the mechanism of precipitate nucleation and growth, particularly in the early stage of phase transformation [68]. On the application side, time-resolved measurements will allow real-time study of synthesis or processing. Some exploratory experiments are already underway, and have demonstrated the feasibility of in situ study of transient behavior during friction stir welding [69]. To fully realize the potential of in situ measurements, further specialized sample test stands, such as controlled-atmosphere furnaces, load-frames, and welding rigs, are needed.

6. Summary and conclusions

Dramatic advances in capabilities are occurring in electron microscopy, atom probe tomography, neutron scattering and X-ray scattering. For electron microscopy, the fine probe sizes of recent aberration-corrected field emission gun instruments represents two to three orders of magnitude increase in electron flux. The point to point resolution of these new aberration corrected microscopes has clearly crossed below the 1 Å barrier. Future activity will include in situ characterization of specimens in a variety of environments that are more representative of real-world applications. For atom probe tomography, the recent instrument advances correspond to two to three orders of magnitude improvement in the rate of data collection. Combined with improvements in specimen preparation techniques, this enables much more rapid analysis of specimens and much higher quantitative precision. The neutron fluxes in the emerging generation of pulsed spallation sources represent an order of magnitude increase compared to existing sources. Improved instrumentation test stands at the reactor and spallation neutron sources can enable a variety of in situ characterization tests to be performed on samples ranging in sizes up to meters. A total of 14 orders of magnitude increase in brilliance has been achieved in the latest synchrotron sources compared to the rotating anode X-ray instruments available in 1960. Test stands available at current synchrotron sources are capable of 3 D analysis of phases and defects in submicron-sized volumes,

and there is active competition to achieve 1 nm nanobeams. Similar to the case for electron microscopy and neutron scattering, there are increasing capabilities at X-ray synchrotron test stands to perform in situ characterization in real-world environments involving application of high temperatures, stresses and other experimental parameters.

Acknowledgements

Research at the Oak Ridge National Laboratory SHaRE User Facility was sponsored by Basic Energy Sciences, U.S. Department of Energy (MKM). SJP would like to thank his collaborators in the work reviewed here, A.R. Lupini, A. Borisevich, Y. Peng, M.P. Oxley, K. van Benthem, M. F. Chisholm, P.D. Nellist, O.L. Krivanek, N. Dellby, M.F. Murfitt, Z.S. Szilagyi, S.F. Findlay and L.J. Allen. We also acknowledge contributions by D.T. Hoelzer, K.F. Russell and D.A. McClintock for the APT results and J.D. Budai for the X-ray results. The electron microscopy, X-ray and neutron scattering research was supported by the Division of Materials Sciences and Engineering, USDOE, and in part by the Laboratory Directed Research and Development Program of ORNL, and by appointments (KvB, AYB, MPO) to the ORNL Postdoctoral Research Program administered jointly by ORNL and ORISE.

References

[1] E.E. Bloom, S.J. Zinkle, F.W. Wiffen, J. Nucl. Mater. 329–333 (2004) 12.
[2] S.J. Zinkle, Phys. Plasma 12 (2005) 058101.
[3] S.J. Zinkle, N.M. Ghoniem, Fus. Eng. Des. 51&52 (2000) 55.
[4] S.J. Zinkle, Fus. Eng. Des. 74 (2005) 31.
[5] D.T. Hoelzer, J. Bentley, M.A. Sokolov, M.K. Miller, G.R. Odette, M.J. Alinger, J. Nucl. Mater. 367–370 (2007) 166.
[6] M. Klimiankou, R. Lindau, A. Moslang, J. Nucl. Mater. 329–333 (2004) 347.
[7] P.M. Rice, S.J. Zinkle, J. Nucl. Mater. 258–263 (1998) 1414.
[8] H. Rose, Ultramicroscopy 56 (1994) 11.
[9] P.E. Batson, N. Dellby, O.L. Krivanek, Nature 418 (2002) 617.
[10] M. Haider, S. Uhlemann, E. Schwan, H. Rose, B. Kabius, K. Urban, Nature 392 (1998) 768.
[11] P.D. Nellist, M.F. Chisholm, N. Dellby, O.L. Krivanek, M.F. Murfitt, Z.S. Szilagyi, A.R. Lupini, A. Borisevich, W.H. Sides, S.J. Pennycook, Science 305 (2004) 1741.
[12] K. Sohlberg, S. Rashkeev, A.Y. Borisevich, S.J. Pennycook, S.T. Pantelides, Chemphyschem 5 (2004) 1893.
[13] P.D. Nellist, S.J. Pennycook, Science 274 (1996) 413.
[14] P.M. Voyles, D.A. Muller, J.L. Grazul, P.H. Citrin, H.J.L. Gossmann, Nature 416 (2002) 826.
[15] A.R. Lupini, S.J. Pennycook, Ultramic 96 (2003) 313.
[16] M. Varela, S.D. Findlay, A.R. Lupini, H.M. Christen, A.Y. Borisevich, N. Dellby, O.L. Krivanek, P.D. Nellist, M.P. Oxley, L.J. Allen, S.J. Pennycook, Phys. Rev. Lett. 92 (2004) 095502.
[17] M. Varela, A.R. Lupini, K. van Benthem, A. Borisevich, M.F. Chisholm, N. Shibata, E. Abe, S.J. Pennycook, Annu. Rev. Mater. Res. 35 (2005) 539.
[18] S.J. Pennycook, A.R. Lupini, M. Varela, A.Y. Borisevich, Y. Peng, M.P. Oxley, K. van Benthem, M.F. Chisholm, in: W. Zhou, Z.L. Wang (Eds.), Scanning Microscopy for Nanotechnology: Techniques and Applications, Springer, 2007.
[19] A.R. Lupini, S.N. Rashkeev, M. Varela, A.Y. Borisevich, M.P. Oxley, K. van Benthem, Y. Peng, N. de Jonge, G.M. Veith, S.T. Pantelides, M.F. Chisholm, S.J. Pennycook, in: A.I. Kirkland, J.L. Hutchison (Eds.), Nanocharacterization, The Royal Society of Chemistry, London, 2007.
[20] O. Scherzer, Z. Phys. 114 (1939) 427.
[21] O. Scherzer, Optik 2 (1947) 114.
[22] J. Zach, M. Haider, Nucl. Instrum. and Meth. A 363 (1995) 316.
[23] A.V. Crewe, J. Wall, J. Langmore, Science 168 (1970) 1338.
[24] N.D. Browning, M.F. Chisholm, S.J. Pennycook, Nature 366 (1993) 143.
[25] G. Duscher, N.D. Browning, S.J. Pennycook, Phys. Status Solidi A 166 (1998) 327.
[26] M. Bosman, K.V. Keast, J.L. Garcia-Munoz, A.J. D'Alfonso, S.D. Findlay, L.J. Allen, Phys. Rev. Lett. 99 (2007) 086102.
[27] K. Kimoto, T. Asaka, T. Nagai, M. Saito, Y. Matsui, K. Ishizuka, Nature 450 (2007) 702.
[28] A.Y. Borisevich, A.R. Lupini, S.J. Pennycook, Proc. Natl. Acad. Sci. USA 103 (2006) 19212.
[29] K. van Benthem, A.R. Lupini, M.P. Oxley, S.D. Findlay, L.J. Allen, S.J. Pennycook, Ultramic 106 (2006) 1062.
[30] A.Y. Borisevich, A.R. Lupini, S. Travaglini, S.J. Pennycook, J. Electron Microsc. 55 (2006) 7.
[31] Y. Matsukawa, Y.N. Osetsky, R.E. Stoller, S.J. Zinkle, J. Nucl. Mater. 351 (2006) 285.
[32] Y. Matsukawa, S.J. Zinkle, Science 318 (2007) 959.
[33] T.F. Kelly, M.K. Miller, Rev. Sci. Instrum. 78 (2007) 031101.
[34] M.K. Miller, Atom Probe Tomography, Kluwer Academic/Plenum, New York, 2000.
[35] M.K. Miller, K.F. Russell, K. Thompson, R. Alvis, D.J. Larson, Microsc. Microanal. 13 (2007) 428.
[36] G.L. Kellogg, T.T. Tsong, J. Appl. Phys. 51 (1980) 1184.
[37] M.K. Miller, P. Angelini, A. Cerezo, K.L. More, J. Phys. 50-C8 (1989) 459.
[38] J.M. Hyde, C.A. English, in: G.E. Lucas, L.L. Snead, M.A. Kirk Jr., R.G. Elliman (Eds.), Microstructural Processes in Irradiated Materials MRS Symp. Proc., vol. 650, Materials Research Society, Pittsburgh, PA, 2001, p. R6.6.1.
[39] M.K. Miller, K.F. Russell, J. Nucl. Mater. 371 (2007) 145.
[40] O.C. Hellman, J.A. Vandenbroucke, J. Rüsing, D. Isheim, D.N. Seidman, Microsc. Microanal. 6 (2000) 437.
[41] G.E. Ice, X-ray Spectrom. 26 (1997) 315.
[42] P. Eisenberger, B.M. Kincaid, Science 200 (1978) 1441.
[43] I.K. Robinson, Phys. Rev. B: Condens. Matter 33 (1986) 3830.
[44] G.E. Ice, C.J. Sparks, A. Habenschuss, L.B. Shaffer, Phys. Rev. Lett. 68 (1992) 863.
[45] H. Stragier, J.O. Cross, J.J. Rehr, L.B. Sorensen, C.E. Bouldin, J.C. Woicik, Phys. Rev. Lett. 69 (1992) 3064.
[46] G.E. Ice, Nucl. Instrum. and Meth. Phys. Res. A 582 (2007) 129.
[47] G.E. Ice, R.I. Barabash, W. Liu, Z. Kristallogr. 220 (2005) 1076.
[48] B.C. Larson, B. Lengeler, MRS Bull. 29 (2004) 152.
[49] H. Reichert, Phys. Rev. Lett. 95 (2005) 235703.
[50] G.E. Ice, B.C. Larson, Adv. Eng. Mater. 2 (2000) 643.
[51] J.D. Budai, M. Yang, B.C. Larson, J.Z. Tischler, W. Liu, H. Weiland, G.E. Ice, Mater. Sci. Forum. 467–470 (2004) 1373.
[52] X.-L. Wang, E.A. Payzant, B. Taljat, C.R. Hubbard, J.R. Keiser, M.J. Jirinec, Mater. Sci. Eng. A 232 (1997) 31.
[53] J.F. Löffler, S. Bossuyt, S.C. Glade, W.L. Johnson, W. Wagner, P. Thiyagarajan, Appl. Phys. Lett. 77 (2000) 525.
[54] M. Bischof, S. Erlach, P. Staron, H. Leitner, C. Scheu, H. Clemons, Z. Metallkd. 96 (2005) 1074.
[55] R. Coppola, R. Lindau, R.P. May, A. Moslang, M. Valli, J. Appl. Crystallogr. 40 (2007) S142.
[56] S.C. Glade, B.D. Wirth, G.R. Odette, P. Asoka-Kumar, J. Nucl. Mater. 351 (2006) 197.
[57] M.K. Miller, B.D. Wirth, G.R. Odette, Mater. Sci. Eng. A 353 (2003) 133.
[58] M. Bischof, P. Staron, A. Michels, P. Granitzer, K. Rumpf, H. Leitner, C. Scheu, H. Clemons, Acta Mater. 55 (2007) 2637.
[59] M.J. Alinger, G.R. Odette, D.T. Hoelzer, J. Nucl. Mater. 329–333 (2004) 382.
[60] M.K. Miller, D.T. Hoelzer, E.A. Kenik, K.F. Russell, Intermetallics 13 (2005) 387.
[61] X.-L. Wang, JOM 58 (March) (2006) 52.
[62] J.R. Keiser, G.B. Sarma, X.-L. Wang, C.R. Hubbard, R.W. Swindeman, D.L. Singbeil, P.M. Singh, Tappi J. 84 (2001) 48.
[63] X.-L. Wang, C.M. Hoffmann, C.H. Hsueh, G.B. Sarma, C.R. Hubbard, J.R. Keiser, Appl. Phys. Lett. 75 (1999) 3294.
[64] T.M. Holden, R.A. Holt, B.M. Powell, J.E. Winegar, Metall. Trans. A 19 (1988) 2207.
[65] B. Clausen, T. Laurentzen, T. Leffers, Acta Mater. 46 (1998) 3087.
[66] Y.D. Wang, H. Tian, A.D. Stoica, X.-L. Wang, P.K. Liaw, J.W. Richardson, Nat. Mater. 2 (2003) 103.
[67] P.K. Liaw, H. Choo, R.A. Buchanan, C.R. Hubbard, X.-L. Wang, Mater. Sci. Eng. A 437 (2006) 126.
[68] X.-L. Wang, T.M. Holden, G.Q. Rennich, A.D. Stoica, P.K. Liaw, H. Choo, C.R. Hubbard, Physica B 386 (2006) 673.
[69] W. Woo, Z. Feng, X.-L. Wang, D.W. Brown, B. Clausen, K. An, H. Choo, C.R. Hubbard, S.A. David, Sci. Technol. Weld. Join. 12 (2007) 298.